Investigation of the toroidal propagation of lithium injected by LIBS into TJ-II plasmas to measure edge ion temperature

B. López-Miranda, F. L. Tabarés, K. J. McCarthy, A. Baciero, D. Tafalla, F. Medina, I. Pastor, A. López-Fraguas, T. Estrada and the TJ-II team

Laboratorio Nacional de Fusión, CIEMAT, Madrid, Spain

Introduction. Wall conditioning is regularly performed in the stellarator TJ-II by glow discharge deposition of boron films and by lithium evaporation from ovens inserted into its vacuum chamber [1]. Recently, in order to test real-time *in-situ* conditioning techniques, a Nd-YAG laser (normally used for Laser Blow-Off [2] and LIBS (Laser-Induced Breakdown Spectroscopy) [3] studies) has been used to ablate lithium off the inner wall of the chamber, this being in line with previous attempts using Li powder droppers [4] or DOLLOP [5]. For this, the laser beam is focussed onto the wall directly opposite its entry window while laser spot power density is controlled by varying the position of a lens outside the chamber.

A well localized Li source, both in position and time, opens up the possibility for transport studies in the plasma periphery. This is possible as laser-ablated Li is quickly ionized by the plasma and thereafter transported along field lines. During the toroidal displacement of Li, collisions with plasma particles lead to the thermalization of the initially cold Li^+ ions. This equilibration process can be followed by time-of-flight (TOF) measurements at different distances from the source. For this, emission monitors (at 548.5 nm for Li^+), AXUV detectors and bolometers are used. The goal here is to demonstrate the viability to study the subsequent toroidal propagation and of Li ablated off the chamber wall by laser ablation in a magnetically confined plasma.

Experimental. The experiments were performed in the TJ-II, a four-period, low magnetic shear stellarator with major and average minor radii of 1.5 m and ≤0.22 m, respectively [6]. Plasmas are generated with H_2 or He as the working gas by ECRH (Electron Cyclotron Resonance Heating) operated at the 2nd harmonic (f = 53.2 GHz, P_{ECRH} <500 kW). A 6-8 ns pulse of a Nd-YAG laser (750 mJ) is used to ablate deposited Li off the inner wall of its vacuum chamber. The ablated Li is ionized rapidly (1st ionization potential is 5.41 eV, 2nd ionization potential is 76.64 eV, ionization rate is 9×10^{-14} m^3 s^{-1} for T_e (edge) of ≈20 eV [6], so ionization time, τ_{ion}, ≈6 μs if n_e(edge) ≈2×10^{18} m^{-3}) by the plasma and is subsequently transported along field lines. This can be seen by following the evolution of neutral and singly ionized Li emission lines for LIBS spectra at different distances toroidally [3]. During their toroidal transport, collisions with plasma particles thermalize the initially cold Li^+ ions. If in equilibrium, measurements of TOF

can be performed at different distances, l, from the source, as shown in Fig. 1 a) at A3, D4, A8, C8, C3, being l=0.67, 1.67, 2.33, 3 and 4.64 m, respectively. For this, light detectors are prepared to select the emission lines at 670.7 nm (Li I) and 548.5 nm (Li II). For monitoring Li I at the source, a ½ m focal length spectrometer (ACTON SpectraPro 500) with a PMT detector (H9305-04 Hamamatsu, Japan) is used. In contrast, for monitoring Li II, a band-pass filter (010FC10-50/5484 by Andover Corp.) and a PMT (R3896 Hamamatsu, Japan) are used. In addition, X-ray monitors (AXUV detectors & Al-1500 Å /C-270 Å filter) and bolometers (unfiltered AXUV detectors, from 5 eV to 5 keV), that collect global plasma radiation, are used to support the experiments.

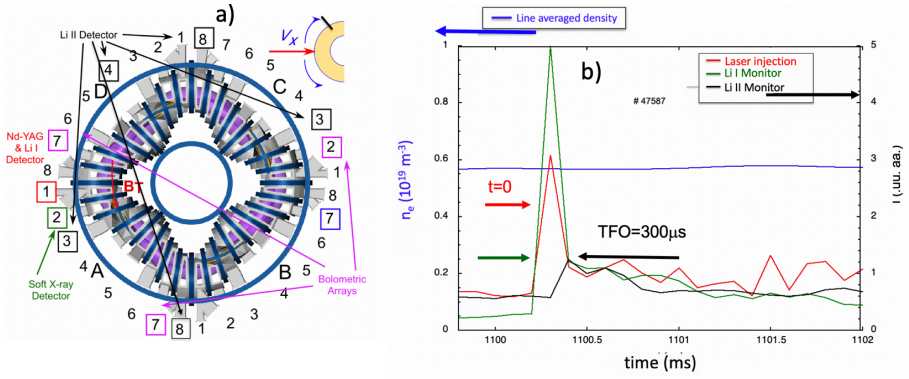

Fig. 1. a) Bird's eye sketch of the TJ-II sectors showing the laser injection point, the X-ray and bolometry detection systems and the different positions of the Li monitor (sectors A3, A8, C3, C8 and D4). b) Line-averaged electron density (blue) and signals from the laser injection (red), Li I monitor (green) and Li II filter (black) for a representative discharge (#47857).

A Maxwellian distribution function $f(v)$ is assumed here for TOF analysis:

$$f(v) = 4\pi \left(\frac{m}{2\pi k T_i}\right)^{3/2} v^2 e^{-\frac{mv^2}{2kT_i}} \tag{1}$$

where m is ion mass, k is Boltzmann´s constant, and T_i is ion temperature. We transform $f(v)$ distribution to $g(t)$ distribution, where t is TOF, $t = l / v$:

$$g(t) = 4\pi \left(\frac{m}{2\pi k T_i}\right)^{3/2} \frac{l^3}{t^4} e^{-\frac{m}{2kT_i}\left(\frac{l}{t}\right)^2} \tag{2}$$

Finally, it is convenient to define the function $h(u)$, where $u = 1/t^2$ as:

$$h(u) = ln\, g(t) + 4\, ln\, t = ln\left(4\pi l^3 \left(\frac{m}{2\pi k T_i}\right)^{3/2}\right) - \frac{m l^2}{2kT_i} u \tag{3}$$

Results and discussion. In order to model a $g(t)$ distribution function profile, a simulation is carried out for different values of T_i from 1 eV to 20 eV for experimental data from discharge #47587. See Fig. 2.a). Here the experimental TOF is considered as the time difference between the lithium injection signal (Li I) and the lithium ion signal (Li II) with l = 2.33 m, *i.e.*, the distance travelled along a field line from sectors A1 to A8. In Fig. 2.a). the function maximum shifts to the right as TOF increases, *i.e.*, as ion temperature, T_i, decreases. In contrast, the

maxima for higher T_i become grouped to the left of this figure and there is reduced separation between them, a region that corresponds to short TOFs, while longer TOFs correspond to lower T_i with greater separation between the maxima. We also plot *h(u)*, whose slope, a straight-line fit, allows us to obtain the experimental T_i. See Fig. 2.b). Two trends are observed here. The 1st slopes, to the left of the figure, are steep and correspond to long TOFs while the 2nd slopes, to the right, are flatter and correspond to shorter TOFs. These are consistent with the simulations in Fig. 2.b). However, it should be noted that the former slopes are subject to greater dispersion and do not reveal the true T_i of the plasma edge. From the latter T_i values obtained are≈25 eV this being very similar to retarding field analyser (RFA) values in TJ-II [7]. The lower values, $T_i \leq 5$ eV, do not correspond to the plasma ions, rather they attributed to the knee-like structure seen in the Li II signal, signal noise or a population of ions in the SOL area. That may be due to a secondary Li^+ ion population (see Fig. 1.a). If the ionization rate for Li^+ is $\approx 10^{-12}$ m^3 s^{-1} for T_e(edge) ≈30 eV [6] and n_e(edge) $\approx 2x10^{18}$ m^{-3}, then τ_{ion} ≈1-2 ms so a significant fraction of the original Li^{+1} population remains in this state. Another feature could be observed by X-ray monitors, which detect a double pass through the same poloidal chord. The differences among the values are higher when the ablation rate increases, maybe due to the reduced amount of ablated Li.

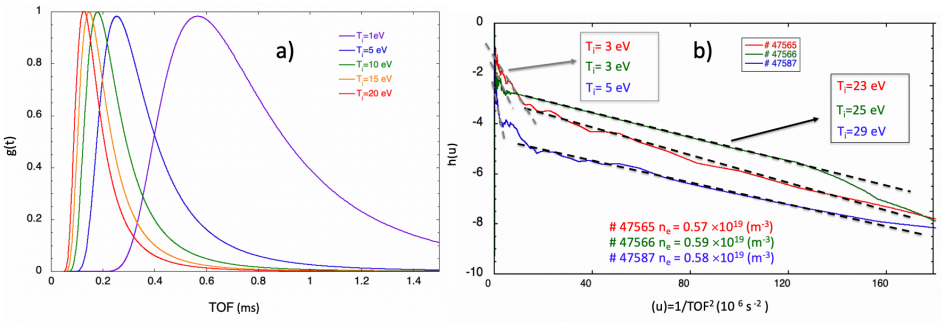

Fig. 2. a) Simulation of the distribution function *g(t)* for different ion temperatures between 1 eV and 20 eV from the signals of the discharge #47587 vs *t*, represented as the experimental TOF. b) Experimental *h(u)* vs $u=1/TOF^2$ distribution functions, in order to obtain the T_i for 3 representative discharges # 47565, # 47566 and # 47587, with H as a working gas and similar line averaged density profiles.

Despite performing a sweep in density to figure out the influence of the radial electric field, E_r , in the T_i measurements, (when a critical density is reached, a spontaneous confinement transition takes place), another experiment will be required because there is not enough data to obtain a definite conclusion. H was changed to He to determine the influence of the working gas in the T_i measure. Here, the density was gradually increased in order to detect a difference in the T_i values. Not only differences in the T_i values obtained with He can be observed in low

density H plasmas, but also, we can observe an increasing in the T_i when the E_r changes its sign, see Fig.3 comparing with the low-density He plasma values (electron-root regimes) [8].

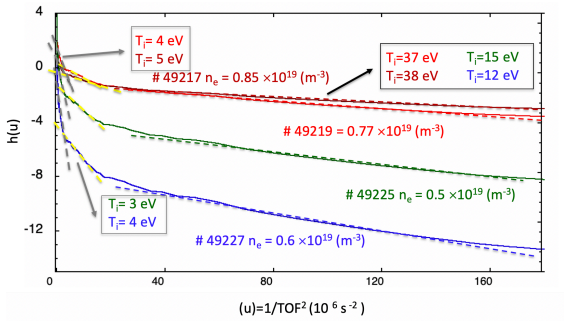

Fig. 3. Experimental *h(u)* vs $u=1/TOF^2$ distributions used to obtain the T_i for He plasmas in electron-root (green & blue) and ion-root (red and brown) regimes. Notice that T_i increases when in ion-root.

Finally, signals from X-ray detectors allow impurity poloidal rotation to be determined. For this work it has been assumed that ion velocity is due solely to the thermalization process. However, if the contribution of ion rotation is considered, the observed velocity, v_x, would be formed by 2 components, one due to ion rotation (v_{rot}) and the other the thermalization velocity (v_{therm}) contribution, hence v_x would be given by:

$$v_x(t) = \frac{l}{t} = v_{rot}(t) + v_{therm}(t) \tag{4}$$

Consequently, $g(t)$function, which allows us, with further analysis, to obtain the TOF, and therefore the T_i , should be written as:

$$g(t) \propto T_i^{-3/2} \left(\frac{l}{t} - v_{rot}\right)^2 e^{-\frac{m\left(\frac{l}{t}-v_{rot}\right)^2}{2KT_i}} \frac{l}{t^2} \tag{5}$$

Conclusions. The viability of injecting Li using LIBS to study ion toroidal propagation has been demonstrated. An original technique to measure T_i at the periphery of fusion plasmas has been developed, where traditionally such measurements have been obtained using passive spectroscopy [9], ion sensitive probes (ISP) [10] or RFA [11]. The values of there T_i are consistent with SOL T_i measured with RFA techniques in TJ-II [12].

This work was partially funded by RTI2018-100835-B-I00 (MCIU/AEI/FEDER, UE). One of the authors (BLM) would like to thank for her scholarship under Grant No. BES-2015-075704.

[1] D. Tafalla *et al*., Fusion Eng. Design **85** 915 (2010)

[2] B. Zurro *et al*., Nucl. Fusion **51** 063015 (2011)

[3] B. López-Miranda *et al*., Rev. Sci. Instrum. **87** 11D811 (2016)

[4] S.M. Kaye *et al*., Nuclear Fusion, **55** 104002 (2015)

[5] D. K. Mansfield *et al*., Nucl. Fusion **41** 12 (2001)

[6] Sánchez J *et al*., J. Nucl. Materials **390** 852 (2009)

[7] I. S. Nedzelskiy *et al*., Problems of Atomic Sci. and Tech. **1** (2009) 174-176.

[8] J. L. Velasco. Plasma Phys. Control. Fusion **55** 124044 (2013)

[9] A. Baciero *et al*., Rev. Sci. Instrum. **72** 971 (2001)

[10] N. E. Zumi *et al*., J. Nucl. Materials **313-316** 696-700 (2003)

[11] R. A. Pitts *et al*., Rev. Sci. Instrum. **74** 11 (2003)

[12] I. S. Nedzelskiy, private communication.